Journal of Alloys and Compounds 504 (2010) 386–390

Contents lists available at ScienceDirect

Journal of Alloys and Compounds

journal homepage: www.elsevier.com/locate/jallcom

# Effects of TiC and TiN addition on combustion synthesis of $Ti_2AlC_{0.5}N_{0.5}$ solid solutions

C.L. Yeh*, C.W. Kuo, F.S. Wu

*Department of Aerospace and Systems Engineering, Feng Chia University, 100 Wenhwa Road, Seatwen, Taichung 40724, Taiwan*

A R T I C L E I N F O

*Article history:*
Received 2 May 2010
Received in revised form 14 May 2010
Accepted 21 May 2010
Available online 4 June 2010

*Keywords:*
Ceramics
X-ray diffraction
$Ti_2AlC_{0.5}N_{0.5}$
Combustion synthesis
Solid solution

A B S T R A C T

Preparation of the solid solution $Ti_2AlC_{0.5}N_{0.5}$ was investigated by self-propagating high-temperature synthesis (SHS) from TiC- and TiN-diluted powder compacts. For the TiC-added samples, combustion reaction was conducted in gaseous nitrogen of 0.45–1.82 MPa. The increase of nitrogen pressure augments the combustion temperature and thus accelerates the reaction front. However, the phase composition of the synthesized product is not affected by the variation of nitrogen pressure, indicating the formation of $Ti_2AlC_{0.5}N_{0.5}$ and three minor phases TiC, TiN, and $Ti_3Al$. For the TiN-containing samples of insufficient nitrogen, the SHS reaction was performed in nitrogen of 0.45 MPa, showing that the increase of the TiN content reduced the combustion temperature and flame-front velocity. Moreover, combustion of the TiN-diluted samples in nitrogen often caused excessive nitridation of the powder compacts. As a result, $Ti_2AlC_{0.5}N_{0.5}$ was yielded along with a substantial amount of secondary phases, including TiN, TiC, and AlN. On the other hand, solid state combustion in Ar was applied for the TiN-added sample at the exact stoichiometry of $Ti_2AlC_{0.5}N_{0.5}$. When compared with combustion synthesis involving gaseous nitrogen, a better phase conversion was achieved by solid state combustion, which produced $Ti_2AlC_{0.5}N_{0.5}$ with negligible amounts of TiC and TiN.

## 1. Introduction

Layered ternary compounds $M_{n+1}AX_n$, where $n = 1$, 2, or 3, M is an early transition metal, A is an A-group (mostly IIIA and IVA) element, and X is either C or N, are a new class of materials which combine many merits of both metals and ceramics [1,2]. Extensive studies have been performed on a number of MAX compounds, including $Ti_3SiC_2$, $Ti_3AlC_2$, $Ti_2AlC$, $Cr_2AlC$, $Ta_2AlC$, and $Ti_2AlN$ [1–10]. In general, MAX carbides and nitrides are readily machinable, good thermal and electrical conductors, relatively soft, thermal shock resistant, damage tolerant, and elastically stiff, and have relatively low thermal expansion coefficients [1–10]. Fabrication of the MAX compounds has been accomplished by a variety of processing routes; for example, hot pressing (HP) [2,3,9], hot isostatic pressing (HIP) [4,8], in situ hot pressing/solid–liquid reaction synthesis [11–15], pulse discharge sintering (PDS) [16–20], and self-propagating high-temperature synthesis (SHS) [21–26].

Furthermore, solid solutions based on the MAX phases can be formed on either the M, A, or X site, which renders great potential for tailoring and/or optimizing the material properties. Many MAX-based solid solutions, like $(Ti,Nb)_2AlC$, $(Cr,V)_2AlC$, $Ti_3(Si,Al)C_2$, $Ti_3(Si,Ge)C_2$, and $Ti_2Al(C,N)$, have been investigated to a great extent [27–36]. Of particular interest for this work is $Ti_2AlC_{0.5}N_{0.5}$, which possesses enhanced properties when compared to two related end members $Ti_2AlC$ and $Ti_2AlN$ [8,32–34]. From the stoichiometric mixtures of Ti, $Al_4C_3$ or Al, AlN, and graphite powders, Barsoum and co-workers [8,32–36] fabricated $Ti_2AlC_{0.5}N_{0.5}$ by hot isostatic pressing at 1300–1400 °C and 40–100 MPa for 10–15 h.

As a promising alternative, combustion synthesis in the SHS mode takes advantage of the self-sustaining merit from highly exothermic reactions, and hence, has the benefits of low energy requirement, short reaction time, and simple facilities [37–40]. The SHS technique not only has been utilized to produce many MAX carbides, like $Ti_3SiC_2$ [21,22], $Ti_3AlC_2$ [23,24], $Ti_2AlC$ [25], and $Ta_2AlC$ [26], but also represents an in situ approach to forming carbonitrides of the transition metals [41–43]. Thus far, combustion synthesis in neither the solid–gas nor solid–solid mode has been applied for the formation of $Ti_2AlC_{0.5}N_{0.5}$. As the first attempt, this study aims to prepare $Ti_2AlC_{0.5}N_{0.5}$ through self-sustaining combustion involving the reaction of TiC- and TiN-diluted samples with gaseous nitrogen. Effects of the diluent content and nitrogen pressure are investigated on the phase composition of the final product, as well as on combustion temperature and propagation velocity of the reaction front. Other than solid–gas combustion, the solid state synthesis is performed with samples composed of Ti, Al, C, and

---

* Corresponding author. Tel.: +886 4 24517250x3963; fax: +886 4 24510862.
*E-mail address:* clyeh@fcu.edu.tw (C.L. Yeh).

0925-8388/$ – see front matter © 2010 Elsevier B.V. All rights reserved.
doi:10.1016/j.jallcom.2010.05.122

**Table 1**
Starting compositions of powder compacts and their corresponding test conditions.

| Diluent | Sample composition | Test environment | Pressure (MPa) |
|---|---|---|---|
| TiC | $1.5Ti + Al + 0.5TiC$ | $N_2$ | 0.45–1.82 |
| TiN | $(2-x)Ti + Al + 0.5C + xTiN$ | $N_2$ for $x = 0.1$–$0.4$ | 0.45 |
| | | Ar for $x = 0.5$ | 0.14 |

TiN powders at the exact stoichiometry of $Ti_2AlC_{0.5}N_{0.5}$ and the resulting products are compared to those synthesized in gaseous nitrogen.

## 2. Experimental methods of approach

Titanium (Strem Chemicals, $\leq$45 µm, 99% purity), aluminum (Showa Chemical Co., $\leq$40 µm, 99% purity), and carbon black (Showa Chemical Co.) powders were used as elemental solid components in this study. A major barricade encountered in the SHS process involving gaseous reagents is that the high combustion temperature tends to melt the powder compact, which reduces the permeability of the sample and thereby hinders the infiltration of the gaseous reactant. Formation of TiN and AlN from the metal powder compacts in nitrogen is the typical example of solid–gas

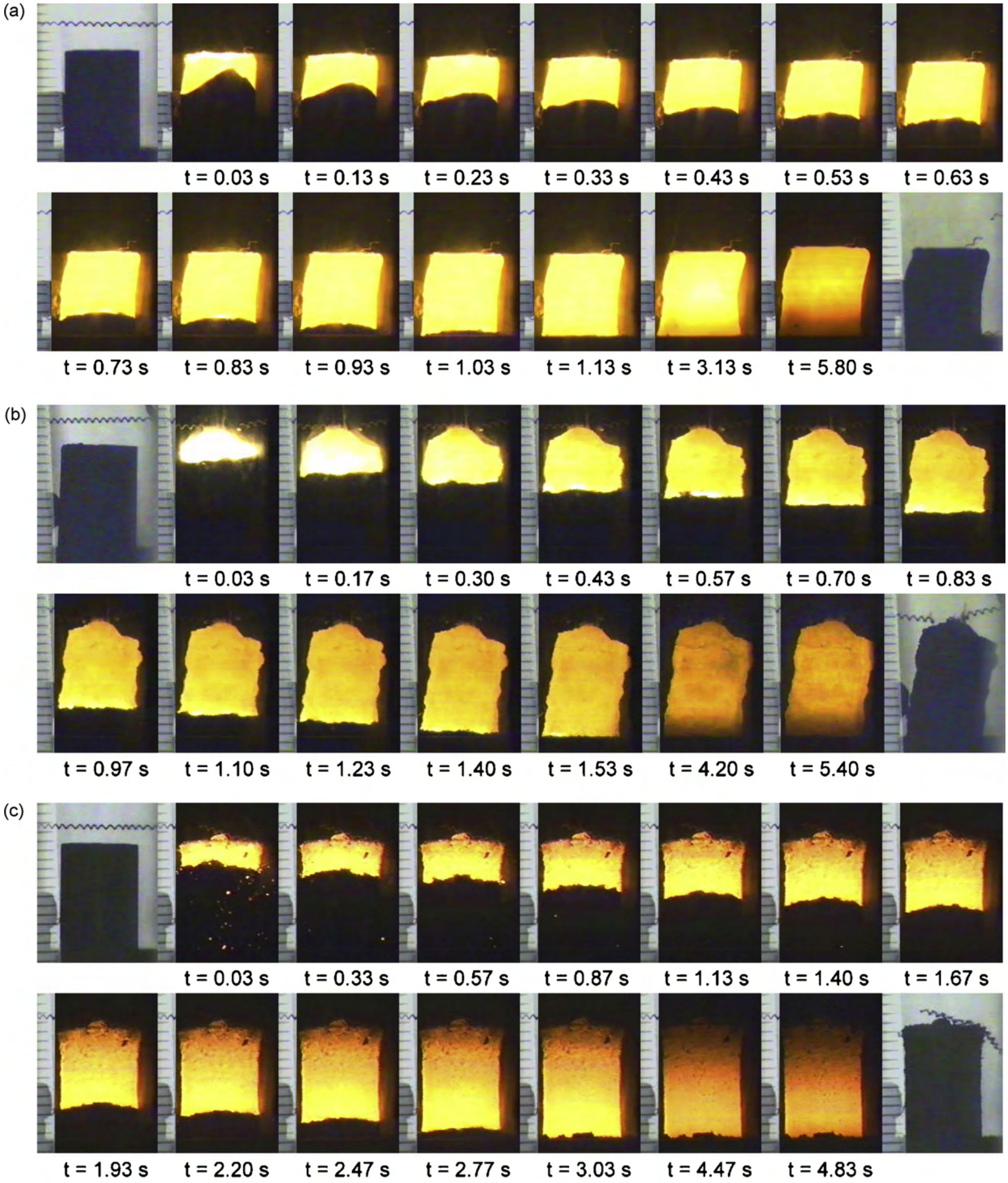

**Fig. 1.** Typical SHS sequences associated with (a) TiC-diluted sample in $N_2$ of 1.14 MPa, (b) TiN-diluted sample with $x = 0.4$ in $N_2$ of 0.45 MPa, and (c) TiN-diluted sample with $x = 0.5$ in Ar of 0.14 MPa.

combustion synthesis [44,45]. Diluting the powder mixture with metal nitrides has been suggested as an effective means to suppress the melting and to improve the degree of nitridation [44,45]. Consequently, this study adopted TiC (Aldrich Chemical, ≤45 μm, 98% purity) and TiN (Strem Chemicals, ≤45 μm, 99% purity) as the diluents to mix with Ti, Al, and carbon powders in a ball mill. The powder blend was then cold-pressed into cylindrical compacts with a diameter of 7 mm, a height of 12 mm, and a compaction density of 55% relative to the theoretical maximum density (TMD).

Table 1 summarizes the starting compositions of TiC- and TiN-diluted powder compacts and their corresponding test environments and pressures. For the TiC-diluted samples, the synthesis reaction was conducted under nitrogen with pressure varying from 0.45 to 1.82 MPa. Combustion of TiN-diluted samples with the stoichiometric parameter $x$ between 0.1 and 0.4 (signifying the TiN content from 2.86 to 11.4 mol%) was performed in nitrogen of 0.45 MPa. When the quantity of TiN in the TiN-added sample increases up to the sample stoichiometry (i.e., $x = 0.5$ or 14.3 mol% TiN) equivalent to that of $Ti_2AlC_{0.5}N_{0.5}$, the SHS process proceeds in the solid state with argon as the surrounding gas. Details of the experimental setup and measurement approach were reported elsewhere [44,45].

## 3. Results and discussion

### 3.1. *Observation of combustion characteristics*

Three recorded combustion sequences illustrating the entire SHS processes associated with formation of $Ti_2AlC_{0.5}N_{0.5}$ from different test configurations are presented in Fig. 1(a)–(c), all of which feature a distinct combustion front propagating in a self-sustaining manner. Fig. 1(a) shows that combustion of a TiC-diluted compact in gaseous nitrogen at 1.14 MPa is accompanied by apparent melting and shrinkage of the burned sample, which is typical of the TiC-added sample igniting in nitrogen and is attributed to the high combustion temperature exceeding the melting point of solid elements. Because nitrogen is normally insufficient within the sample compact, continuous infiltration of nitrogen gas after the passage of the combustion wave leads to subsequent nitridation and prolonged combustion luminosity for about 2–3 s. For the TiN-diluted samples with $x = 0.1$–$0.4$, the SHS process in nitrogen of 0.45 MPa also caused melting and deformation of the powder compacts. However, the extent of sample melting was reduced with increasing TiN content due to the decrease of the reaction temperature. As revealed in Fig. 1(b), a mild degree of melting is observed for the TiN-added sample with $x = 0.4$.

In contrast to the SHS process of the solid–gas mode under nitrogen, Fig. 1(c) presents solid state combustion of the TiN-containing sample with $x = 0.5$ in argon. The burned sample essentially retains its original shape and the combustion wave propagates at a slower rate when compared to those shown in Fig. 1(a) and (b). This could be caused by the fact that the reaction of Ti with carbon to form TiC (with the enthalpy of formation $\Delta H_f = -184.1$ kJ/mol) plays the major role of heat release in the sample subjected to solid state combustion, which is less exothermic than that of Ti with nitrogen to yield TiN ($\Delta H_f = -337.7$ kJ/mol) for solid–gas combustion of the TiC- and TiN-diluted powder compacts under nitrogen [46].

### 3.2. *Measurement of flame-front propagation velocity and combustion temperature*

The influence of nitrogen pressure on the propagation velocity of the combustion front ($V_f$) of the TiC-diluted powder compact is presented in Fig. 2. The combustion velocity increases from 5.3 to 6.9 mm/s with increasing nitrogen pressure, on account of a higher concentration of nitrogen in the reaction front. Two data points plotted in Fig. 2 under the same test condition represent two independent measurements in order to confirm the accuracy of measured values. For the TiN-diluted samples, Fig. 3 shows a substantial decrease in the reaction front velocity from 7.6 to 2.9 mm/s as the content of TiN increases. This can be explained by the dilution effect of TiN on combustion. It should be noted that the lowest flame-front velocity reported in Fig. 3 was detected from the sample subjected to solid state combustion in argon. The weak exothermicity of solid state combustion, as mentioned above, could be the other reason for such a low reaction rate.

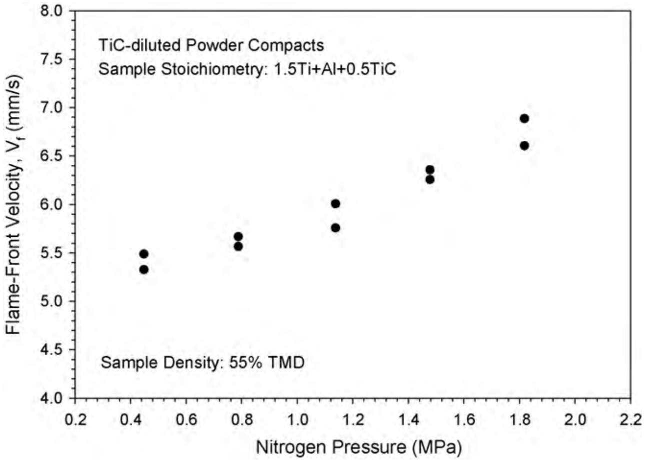

**Fig. 2.** Effect of nitrogen pressure on flame-front propagation velocity of TiC-diluted powder compacts.

Fig. 4 depicts three temperature profiles recorded from combustion of the TiC-diluted samples in nitrogen. The abrupt rise in temperature signifies rapid arrival of the combustion wave. The peak value corresponds to the flame-front temperature. After the passage of the combustion wave, the sample temperature essentially reaches a plateau and then declines slowly. The presence of a nearly flat section in the temperature profile could be a consequence of the afterburning reaction resulting from continuous penetration of nitrogen gas into the sample. The decrease of temperature was largely caused by the heat loss to the surroundings. In agreement with pressure dependence of the flame-front velocity, the combustion front temperature increases from about 1430 to 1700 °C with increasing pressure of nitrogen.

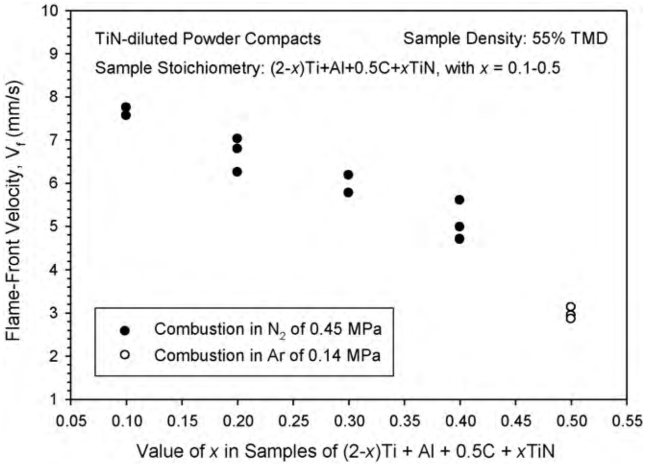

**Fig. 3.** Effect of TiN content on flame-front propagation velocity of TiN-diluted powder compacts.

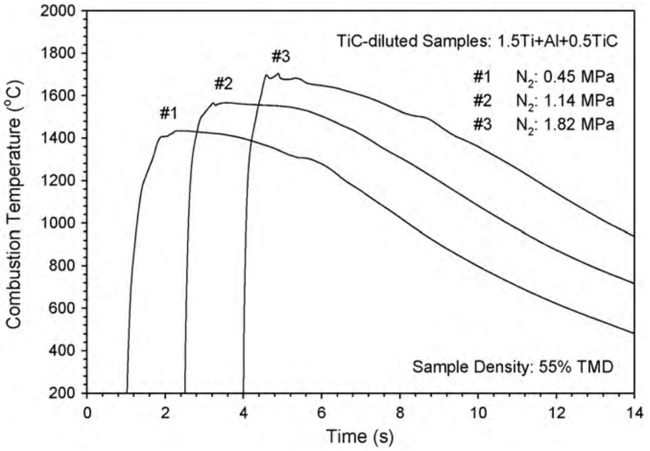

**Fig. 4.** Effect of nitrogen pressure on combustion temperature of TiC-diluted powder compacts.

For the TiN-diluted samples under nitrogen of 0.45 MPa, Fig. 5 shows a reduction in the combustion temperature for the sample with a higher content of TiN. Similar to those of Fig. 4, the temperature profiles (#2 and #3 of Fig. 5) associated with solid–gas combustion exhibit a nearly plateau region following the surging spike, suggestive of existence of the afterburning reaction. The intersection of curves #2 and #3 in Fig. 5 is mainly caused by the fact that the afterburning reaction taking place in the sample of $x = 0.3$ last a longer duration. For the sample containing TiN at $x = 0.5$, the synthesis reaction proceeds in the solid state and the reaction front temperature (profile #1) reaches barely 1200 °C that confirms its weak exothermicity. Moreover, the temperature profile indicates no prolonged afterburning reactions.

### 3.3. Composition analysis of combustion products

Typical XRD patterns of the products synthesized from TiC-diluted compacts in nitrogen of different pressures are presented in Fig. 6(a)–(c), within which $Ti_2AlC_{0.5}N_{0.5}$ is identified as the dominant phase along with trivial amounts of secondary components including TiN, TiC, and $Ti_3Al$. According to Fig. 6(a)–(c), the variation of nitrogen pressure produced almost no effects on the product composition. This could be caused by that fact that melting of the reactant compact limits the infiltration of nitrogen. As a result, the amounts of nitrogen uptake are comparable for the samples under different pressures of nitrogen. The presence of the intermetallic phase $Ti_3Al$ signifies the interaction between Ti and Al. It is believed that $Ti_3Al$ reacts subsequently with Al to yield TiAl an important intermediate in the evolution of $Ti_2AlC$ and $Ti_2AlN$ [47,15], from both of which the solid solution $Ti_2AlC_{0.5}N_{0.5}$ is formed.

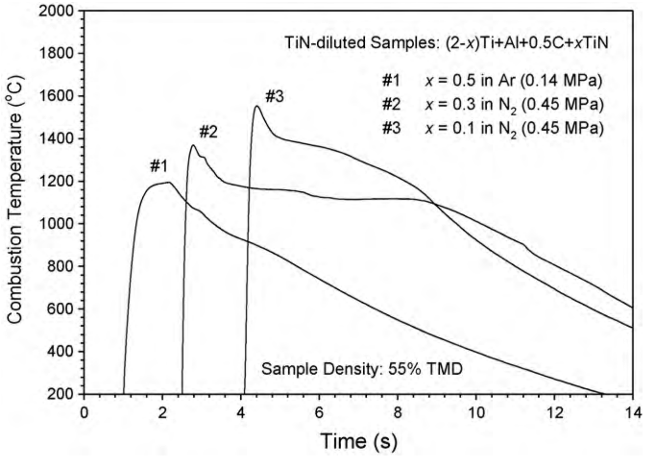

**Fig. 5.** Effect of TiN content on combustion temperature of TiN-diluted powder compacts.

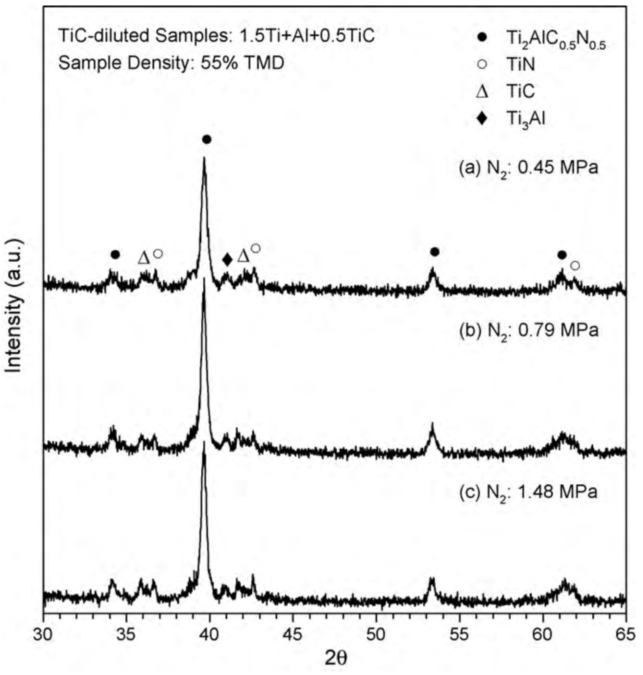

**Fig. 6.** XRD patterns of products synthesized from TiC-diluted samples in (a) $N_2$: 0.45 MPa, (b) $N_2$: 0.79 MPa, and (c) $N_2$: 1.48 MPa.

For the TiN-diluted sample of $x = 0.2$ in nitrogen of 0.45 MPa, Fig. 7(a) shows the product composed of similar phase composition to that obtained from the TiC-added sample presented in Fig. 6, but indicates the higher content of secondary components, especially TiN. As the sample is diluted by TiN at $x = 0.4$, Fig. 7(b) reveals the increase of TiN and the presence of AlN in the final product. Fig. 7(a)

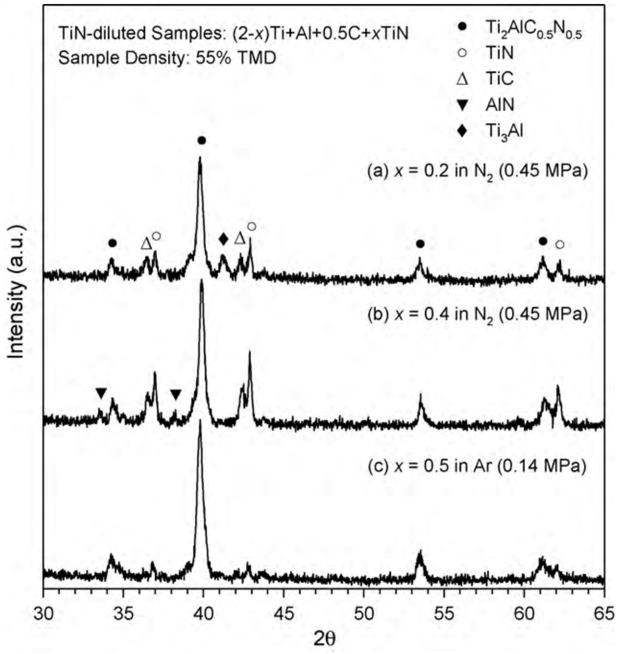

**Fig. 7.** XRD patterns of products synthesized from TiN-diluted samples with (a) $x = 0.2$ in $N_2$ (0.45 MPa), (b) $x = 0.4$ in $N_2$ (0.45 MPa), and (c) $x = 0.5$ in Ar (0.14 MPa).

**Table 2**
Summary of phase composition of SHS products with respect to their initial stoichiometries and test conditions.

| Test sample | Test environment (pressure, MPa) | Phase composition of SHS products | |
|---|---|---|---|
| | | Dominant phase | Sceondary phases |
| TiC-diluted samples | $N_2$ (0.45–1.82) | $Ti_2AlC_{0.5}N_{0.5}$ | TiC, TiN, $Ti_3Al$ |
| TiN-diluted samples | | | |
| $x = 0.1$ and 0.2 | $N_2$ (0.45) | $Ti_2AlC_{0.5}N_{0.5}$ | TiC, TiN, $Ti_3Al$ |
| $x = 0.3$ and 0.4 | $N_2$ (0.45) | $Ti_2AlC_{0.5}N_{0.5}$ | TiC, TiN, AlN |
| $x = 0.5$ | Ar (0.14) | $Ti_2AlC_{0.5}N_{0.5}$ | TiC, TiN |

and (b) implies excessive nitridation occurring in solid–gas combustion of the TiN-diluted powder compacts under nitrogen. On the other hand, Fig. 7(c) shows the formation of $Ti_2AlC_{0.5}N_{0.5}$ along with two minor phases, TiN and TiC, of negligible amounts from solid state combustion of the TiN-added sample with $x = 0.5$. As indicated by Fig. 7(a)–(c), for the TiN-added samples solid state combustion represents a more favorable route to prepare $Ti_2AlC_{0.5}N_{0.5}$ than solid–gas combustion.

Table 2 summarizes the phase composition of the end products with respect to their initial sample stiochiometries and test conditions. The solid solution $Ti_2AlC_{0.5}N_{0.5}$ dominates in all final products, but secondary phases vary with test configurations. In addition to TiC and TiN, $Ti_3Al$ was observed in the products obtained from both TiC-added samples and TiN-diluted compacts with $x = 0.1$ and 0.2. When the TiN content in the samples arrived at $x = 0.3$ and 0.4, AlN was formed in the final products.

## 4. Conclusions

Preparation of solid solution $Ti_2AlC_{0.5}N_{0.5}$ was conducted by the SHS process in either the solid–gas or solid–solid mode. For combustion synthesis involving gaseous nitrogen, TiC- and TiN-diluted samples were adopted. Besides, $Ti_2AlC_{0.5}N_{0.5}$ was fabricated through solid state combustion with green samples composed of Ti, Al, C, and TiN at the exact stoichiometry of $Ti_2AlC_{0.5}N_{0.5}$.

During the SHS process under nitrogen of 0.45–1.82 MPa, TiC-diluted powder compacts experienced substantial melting because of the high combustion temperature, which increases with nitrogen pressure. The variation of the reaction front velocity with nitrogen pressure was found to be in a manner consistent with that of combustion temperature. However, the increase of nitrogen pressure had almost no effects on the phase composition of the end product, implying comparable nitrogen uptake from solid–gas combustion. Based upon the XRD analysis, the solid solution $Ti_2AlC_{0.5}N_{0.5}$ is identified as the dominant component in the final products that contain three minor phases, TiC, TiN, and $Ti_3Al$.

For the TiN-diluted powder compacts undergoing solid–gas combustion in nitrogen of 0.45 MPa, the extent of sample melting was reduced by increasing the mole fraction of TiN from 2.86 to 11.4 mol%. Moreover, the combustion temperature and flame-front velocity decreased with increasing TiN content. Despite the fact that $Ti_2AlC_{0.5}N_{0.5}$ was formed as the major constituent, excessive nitridation was observed in the samples diluted by high contents of TiN, especially in the cases of $x = 0.3$ and 0.4, which led to a great amount of TiN and the formation of AlN in the end products. In contrast, solid state combustion of the TiN-added sample with $x = 0.5$ (14.3 mol% TiN) significantly improves the phase conversion and produces $Ti_2AlC_{0.5}N_{0.5}$ with negligible amounts of TiC and TiN.

## Acknowledgement

This research was sponsored by the National Science Council of Taiwan, ROC, under the grant of NSC 98-2221-E-035-065-MY2.

## References

[1] M.W. Barsoum, Prog. Solid State Chem. 28 (2000) 201–281.
[2] M.W. Barsoum, D. Brodkin, T. El-Raghy, Scr. Mater. 36 (5) (1997) 535–541.
[3] M.W. Barsoum, T. El-Raghy, J. Am. Ceram. Soc. 79 (7) (1996) 1953–1956.
[4] N.V. Tzenov, M.W. Barsoum, J. Am. Ceram. Soc. 83 (4) (2000) 825–832.
[5] J.Y. Wang, Y.C. Zhou, Annu. Rev. Mater. Res. 39 (2009) 415–443.
[6] H.B. Zhang, Y.W. Bao, Y.C. Zhou, J. Mater. Sci. Technol. 25 (2009) 1–38.
[7] Z.J. Lin, M.J. Zhuo, Y.C. Zhou, M.S. Li, J.Y. Wang, Acta Mater. 54 (2006) 1009–1015.
[8] M.W. Barsoum, M. Ali, T. El-Raghy, Metall. Mater. Trans. 31A (2000) 1857–1865.
[9] W.B. Tian, P.L. Wang, G.J. Zhang, Y.M. Kan, Y.X. Li, D.S. Yan, Scr. Mater. 54 (2006) 841–846.
[10] J. Lis, L. Chlubny, M. Łopaciński, L. Stobierski, M.M. Bućko, J. Eur. Ceram. Soc. 28 (2008) 1009–1014.
[11] X.H. Wang, Y.C. Zhou, Acta Mater. 50 (2002) 3141–3149.
[12] X.H. Wang, Y.C. Zhou, Z. Metallkd. 93 (1) (2002) 66–71.
[13] Z.J. Lin, Y.C. Zhou, M.S. Li, J.Y. Wang, Z. Metallkd. 96 (3) (2005) 291–296.
[14] C. Hu, L. He, J. Zhang, Y. Bao, J.Y. Wang, M.S. Li, Y.C. Zhou, J. Eur. Ceram. Soc. 28 (2008) 1679–1685.
[15] Z.J. Lin, M.J. Zhuo, M.S. Li, J.Y. Wang, Y.C. Zhou, Scr. Mater. 56 (2007) 1115–1118.
[16] Z.F. Zhang, Z.M. Sun, H. Hashimoto, T. Abe, J. Eur. Ceram. Soc. 22 (2002) 2957–2961.
[17] Z.M. Sun, S. Yang, H. Hashimoto, J. Alloys Compd. 439 (2007) 321–325.
[18] Y. Zou, Z.M. Sun, H. Hashimoto, S. Tada, J. Alloys Compd. 456 (2008) 456–460.
[19] Y. Zou, Z.M. Sun, H. Hashimoto, L. Cheng, J. Alloys Compd. 468 (2009) 217–221.
[20] W.B. Tian, Z.M. Sun, Y.L. Du, H. Hashimoto, Mater. Lett. 63 (2009) 670–672.
[21] C.L. Yeh, Y.G. Shen, J. Alloys Compd. 458 (2008) 286–291.
[22] C.L. Yeh, Y.G. Shen, J. Alloys Compd. 461 (2008) 654–660.
[23] C.L. Yeh, Y.G. Shen, J. Alloys Compd. 466 (2008) 308–313.
[24] C.L. Yeh, Y.G. Shen, J. Alloys Compd. 473 (2009) 408–413.
[25] C.L. Yeh, Y.G. Shen, J. Alloys Compd. 470 (2009) 424–428.
[26] C.L. Yeh, Y.G. Shen, J. Alloys Compd. 482 (2009) 219–223.
[27] I. Salama, T. El-Raghy, M.W. Barsoum, J. Alloys Compd. 347 (2002) 271–278.
[28] W.B. Tian, Z.M. Sun, H. Hashimoto, Y.L. Du, J. Alloys Compd. 484 (2009) 130–133.
[29] Y.C. Zhou, J.X. Chen, J.Y. Wang, Acta Mater. 54 (2006) 1317–1322.
[30] D.B. Lee, T.D. Nguyen, S.W. Park, J. Alloys Compd. 469 (2009) 374–379.
[31] A. Ganguly, T. Zhen, M.W. Barsoum, J. Alloys Compd. 376 (2004) 287–295.
[32] M. Radovic, A. Ganguly, M.W. Barsoum, J. Mater. Res. 23 (2008) 1517–1521.
[33] T. Scabarozi, A. Ganguly, J.D. Hettinger, S.E. Lofland, S. Amini, P. Finkel, T. El-Raghy, M.W. Barsoum, J. Appl. Phys. 104 (2008) 073713.
[34] Y.L. Du, Z.M. Sun, H. Hashimoto, M.W. Barsoum, Phys. Lett. A 374 (2009) 78–82.
[35] A.G. Zhou, M.W. Barsoum, J. Alloy Compd. (2010), doi:10.1016/j.jallcom.2010.03.099.
[36] M.K. Drulis, H. Drulis, A.E. Hackemer, A. Ganguly, T. El-Raghy, M.W. Barsoum, J. Alloys Compd. 433 (2007) 59–62.
[37] A.G. Merzhanov, J. Mater. Process. Technol. 56 (1996) 222–241.
[38] Z.A. Munir, U. Anselmi-Tamburini, Mater. Sci. Rep. 3 (1989) 277–365.
[39] C.L. Yeh, in: K.H.J. Buschow, R.W. Cahn, M.C. Flemings, E.J. Kramer, S. Mahajan, P. Veyssiere (Eds.), Encyclopaedia of Materials: Science and Technology, Elsevier, Amsterdam, 2010.
[40] C.L. Yeh, in: M. Lackner (Ed.), Combustion Synthesis – Novel Routes to Novel Materials, Bentham Science, 2010.
[41] C.L. Yeh, Y.D. Chen, Ceram. Int. 31 (2005) 719–729.
[42] C.L. Yeh, E.W. Liu, Ceram. Int. 32 (2006) 653–658.
[43] C.L. Yeh, Y.D. Chen, Ceram. Int. 33 (2007) 365–371.
[44] C.L. Yeh, H.C. Chuang, Ceram. Int. 30 (2004) 705–714.
[45] C.L. Yeh, E.W. Liu, J. Alloys Compd. 433 (2007) 147–153.
[46] M. Binnewies, E. Milke, Thermochemical Data of Elements and Compounds, Wiley-VCH Verlag GmbH, Weinheim, New York, 2002.
[47] G. Liu, K. Chen, H. Zhou, J. Guo, K. Ren, J.M.F. Ferreira, Mater. Lett. 61 (2007) 779–784.